

From Single to Multiple-Photon Decoherence in an Atom Interferometer

David A. Kokorowski, Alex D. Cronin, Tony D. Roberts, and David E. Pritchard
Massachusetts Institute of Technology, Cambridge, MA 02139
(December 2, 2024)

We measure the decoherence of a spatially separated atomic superposition due to spontaneous photon scattering. We observe a qualitative change in decoherence versus separation as the number of scattered photons increases, and verify quantitatively the decoherence rate constant in the many-photon limit. Our results illustrate an evolution of decoherence consistent with general models developed for a broad class of decoherence phenomenon.

03.65.Bz,03.75.Dg

Decoherence is the result of entanglement between a quantum system and an unobserved environment, and manifests as the reduction of coherent superpositions into incoherent mixtures. This reduction occurs more quickly as the number of particles comprising a quantum system increases, establishing decoherence as a fundamental limit to large-scale quantum computation [1] and communication [2]. Progress in these fields therefore relies upon understanding and correcting for decoherence effects. On a macroscopic scale, decoherence is unavoidable and explains the emergence of classical behavior in a world governed by quantum mechanical laws.

Theoretical treatments of decoherence provide a description (typically a master equation) for the evolution of a system's density matrix under the influence of a specific environment. For spatial decoherence, various environments including a thermal bath of harmonic oscillators [3], a scalar field [4], and an isotropic distribution of scatterers [5,6] have been studied. In the high-temperature or many scatterer limit, these models all yield a diffusion-like master equation for the system's spatial density matrix, $\rho(x, x')$:

$$\frac{d\rho}{dt} = -\frac{i}{\hbar} [H, \rho] - D^2 |x - x'|^2 \rho, \quad (1)$$

where H is the Hamiltonian for the isolated system and D , the diffusion constant, depends on the details of the system-environment coupling. Assuming negligible internal dynamics, this equation predicts an exponential reduction in coherence with time and with separation squared:

$$\rho(x, x', t) = e^{-D^2 |x - x'|^2 t} \rho(x, x', 0). \quad (2)$$

To investigate this behavior experimentally, we have studied the loss of spatial coherence of atoms within an atom interferometer due to spontaneous scattering of a variable number of photons. In the many photon limit,

this system and environment are a simple case of the general models above and we observe decoherence consistent with Eq. (2). Decoherence in the few photon limit is of a qualitatively different character, and we have followed the smooth transition between these two regimes.

The atom interferometer [7] is realized by passing a collimated, supersonic beam of Na atoms (velocity ≈ 3000 m/s using a He carrier gas) through three diffraction gratings arranged in the Mach-Zehnder geometry (Fig. 1). Prior to the first grating, the atoms are collimated and optically pumped into the $^3S_{\frac{1}{2}}|F = 2, m_f = +2\rangle$ ground state. Two paths through the interferometer, separated by up to $20\mu\text{m}$, overlap at the position of the third grating, forming a spatial interference pattern with the same period (200 nm) as the gratings. This pattern is masked by the third grating and the total transmitted flux is detected using a $50\mu\text{m}$ hot wire. The interference pattern is measured as an oscillating atomic flux versus grating position. Because the contrast of the interference pattern is proportional to the coherence between the two paths, reduction in contrast is direct evidence of decoherence.

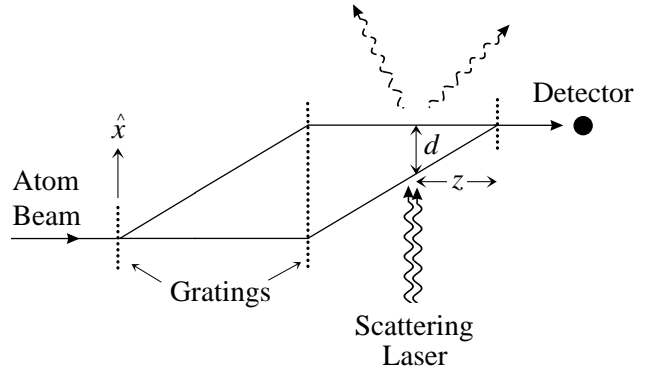


FIG. 1. A schematic of our apparatus: a Mach-Zehnder interferometer comprised of three, evenly spaced, transmission gratings. Within the interferometer, sodium atoms continuously absorb and spontaneously emit photons from a variable intensity laser beam. Decoherence due to spontaneous emission is measured as a reduction in contrast of the interference fringes.

The decohering environment we study consists of photons from a laser beam directed along the \hat{x} axis which intersects both interfering paths. The circularly polarized laser light is tuned to the $^3S_{\frac{1}{2}}|2, +2\rangle \rightarrow ^3P_{\frac{3}{2}}|3, +3\rangle$ transition with wavelength $\lambda = 2\pi/k_0 = 590$ nm. Because the atoms are dipole forbidden from decaying to any state other than $^3S_{\frac{1}{2}}|2, +2\rangle$, they can continuously

scatter photons without falling out of resonance (the natural linewidth is ~ 200 photon recoils wide).

At the intersection of the atomic beam and scattering laser, each atom's transverse wavefunction is peaked at two positions which we label x and $x + d$. If a photon, initially in momentum state $|k_0\rangle$, scatters from this atom, the two become entangled:

$$|\psi\rangle_i = (|x\rangle + |x + d\rangle) \otimes |k_0\rangle \xrightarrow{\text{scat.}} |x\rangle \otimes |\phi_x\rangle + |x + d\rangle \otimes e^{ik_0 d} |\phi_{x+d}\rangle, \quad (3)$$

where $|\phi_x\rangle$ is the wavefunction of a photon spontaneously emitted from position x and the factor $e^{ik_0 d}$ in accounts for the difference in spatial phase of the initial photon at the two positions. Generalizing the entangled wavefunction in Eq. 3 to a density matrix and tracing over a basis of scattered photon states, the net effect of scattering on the atom's spatial coherence is:

$$\rho(x, x + d) \xrightarrow{\text{scat.}} \rho(x, x + d) \beta(d), \quad (4)$$

where $\beta(d)$ is known as the decoherence function and has the properties $|\beta(d)| \leq 1$ and $\beta(0) = 1$. The decoherence function thus defined is equal to the inner product of the two final photon states, which are identical apart from an overall translation:

$$\begin{aligned} \beta(d) &= e^{ik_0 d} \langle \phi_x | \phi_{x+d} \rangle = e^{ik_0 d} \langle \phi_x | e^{-i \hat{k}_x d} | \phi_x \rangle \\ &= \int d\Delta k P(\Delta k) e^{-i \Delta k d}, \end{aligned} \quad (5)$$

where the operator \hat{k}_x is the generator of photon translations along the \hat{x} axis. The resulting decoherence function is the Fourier transform of the probability distribution $P(\Delta k)$, where $\Delta k = k_x - k_0$ is the change in momentum of the photon along the \hat{x} axis.

Previous experiments [8,9] have measured the decoherence function for an atom which spontaneously scatters a single photon. The theoretical prediction which these experiments confirm is displayed as the solid line in Fig. 2. Beneath an overall decay in coherence with distance, periodic coherence revivals are observed. This shape follows directly from the Fourier transform of the dipole radiation pattern for spontaneous emission. It may also be explained in terms of the ability of a single photon to provide which-path information [9]: the contrast drops to zero when the path separation is approximately equal to the resolving power of an ideal Heisenberg microscope $d \approx \lambda/2$, with revivals resulting from path ambiguity due to diffraction structure in the image.

We now proceed to measure the decoherence function appropriate for multiple photon scattering events. If several photons are scattered, and if successive scattering events are independent, the total decoherence function includes one factor of β for each scattered photon:

$$\beta_{\text{total}}(d) = \sum_{n=0}^{\infty} P(n) \beta^n(d). \quad (6)$$

In our experiment, the total number of photons scattered by an individual atom is intrinsically uncertain, but is described by the distribution $P(n)$ which can be measured or calculated. The sum in Eq. (6) is a trace over this additional degree of freedom of the environment.

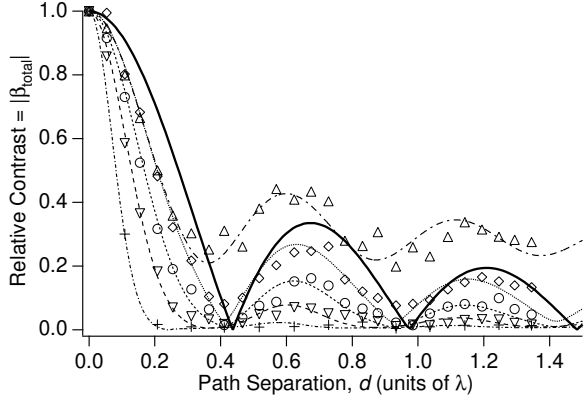


FIG. 2. The total decoherence function, $|\beta_{\text{total}}|$, measured as the normalized contrast after spontaneous photon scattering. The solid line is the single photon decoherence function. Also displayed are the best fits from which we determine $\bar{n} = 0.9$ (\triangle), 1.4 (\diamond), 1.8 (\circ), 2.6 (∇), and 8.2 ($+$).

Figure 2 shows measurements of the decoherence function for a series of laser intensities corresponding to an average number of scattered photons, \bar{n} , ranging from ~ 1 to ~ 8 . At each intensity, a reference contrast and phase was measured, with the scattering laser positioned such that the interfering paths were overlapped ($d = 0$). We then adjusted the longitudinal position of the scattering laser, z , to select specific path separations in the range $0 < d < 1.4\lambda$ at which to measure the decoherence function (see Fig. 1). For each path separation, the ratio of the measured atom interference contrast to the reference contrast yields the magnitude of the decoherence function, $|\beta_{\text{total}}(d)|$. Similarly, the difference between the measured atom interference phase and the reference phase yields the phase of the decoherence function.

We fit the data using Eq. (6) and taking $P(n) \simeq \exp(-\frac{1}{2}(n - \bar{n})^2/\sigma_n^2)$. This form was chosen as a good approximation to Monte-Carlo Wavefunction calculations of $P(n)$ for our laser parameters. From the best fit curves displayed in Fig. 2, values were extracted for \bar{n} and σ_n which were consistent with, and more accurate than, independent measurements of $P(n)$ based on the deflection and broadening of the atomic beam with the scattering laser blocked versus unblocked.

In the regime $d \gg \lambda$, a single scattered photon suffices to completely destroy the coherence between paths. Thus, the non-zero asymptotic value (for $\bar{n} = 0.9$ in Fig. 2) of the decoherence function at large path separation is equal to the fraction of atoms which scatter zero photons (i.e. decoherence is proportional to the atom-photon interaction cross-section). In essence, only the forward

scattered portion of the atomic wavefunction contributes to the interference signal. This phenomenon is a simple example of ‘‘saturation’’ of decoherence [6,10]: the loss of coherence becomes independent of path separation at a characteristic length scale of the environment. Cheng and Raymer [11] have demonstrated another type of saturation in a laser interferometer in which both paths pass through a disordered collection of polystyrene microspheres. Their experiment exhibits features similar to our own: the decoherence was observed to saturate when the path separation reached roughly the diameter of the microspheres, and the asymptotic decoherence rate was proportional to the microsphere-light scattering cross section.

As the average number of scattered photons increases, the overall amount of decoherence increases, and the contrast revivals disappear. This behavior can be formalized as the Fourier transform of the total momentum distribution of all scattered photons:

$$\beta^n(d) = \int d\Delta K P(\Delta K) e^{i\Delta K d}, \quad (7)$$

where $\Delta K = \sum_{i=1}^n \Delta k_i$. As $n \rightarrow \infty$, the central limit theorem predicts that $P(\Delta K)$ will tend towards a Gaussian with mean nk_0 and variance $n\sigma_k^2$ (where $\sigma_k = \frac{2}{5}k_0$ is the rms transverse momentum of an emitted photon). Indeed, in the case of spontaneous emission, $P(\Delta k)$ is already approximately Gaussian for $n > 3$. In this limit the decoherence function reduces to:

$$\begin{aligned} \beta^n(d) &= \int d\Delta K \left[e^{-\frac{1}{2}(\Delta K - nk_0)^2/n\sigma_k^2} \right] e^{i\Delta K d} \quad (8) \\ &= e^{-\frac{1}{2}n\sigma_k^2 d^2} e^{-in k_0 d}. \end{aligned}$$

Inserting this expression into Eq. (6) and taking $d/\lambda \ll 1$, we find:

$$\lim_{\bar{n} \rightarrow \infty} \beta_{\text{total}}(d) = e^{-\frac{1}{2}\kappa^2 d^2} e^{-i\bar{n} k_0 d}, \quad (9)$$

where

$$\kappa^2 = \bar{n}\sigma_k^2 + \sigma_n^2 k_0^2 \quad (10)$$

is the variance of the total momentum transferred to the atom from the scattered photons. The first term in Eq. (10) comes from the trace over modes available to the spontaneously emitted photon, while the second is related to the uncertainty in number of absorbed photons combined with the fixed phase $k_0 d$ imparted by each.

If $\sigma_n = \sqrt{\bar{n}}$ (i.e. Poissonian statistics), Eq. (9) predicts an exponential decay in contrast with number of scattered photons ($\kappa^2 \propto \bar{n}$). If in addition the scattering rate, Γ , is constant, then $\bar{n} = \Gamma t$ and the decoherence has exactly the exponential form derived from a master equation of the type given in Eq. (1).

We have measured this exponential decay of coherence of an ensemble of identically prepared atoms by varying the average number of scattered photons, leaving the

path separation fixed (Fig. 3). Theory curves (solid lines) are based on Eq. (9) with σ_n determined from the broadening of the atomic beam due to the momentum of the scattered photons. The product of the two remaining free parameters, $\bar{n}d$, was obtained from the phase of the decoherence function (equal to the phase shift of the measured interference pattern).

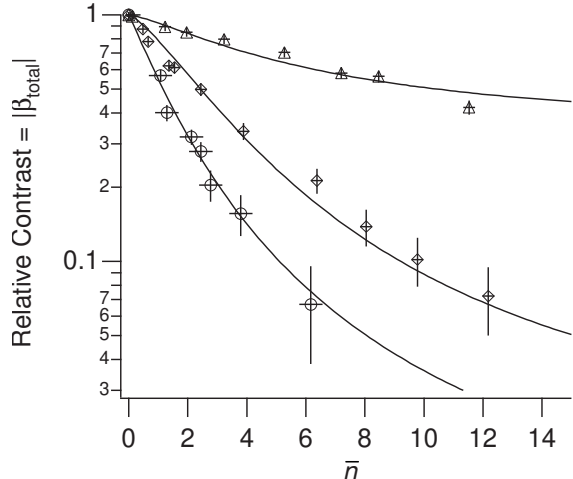


FIG. 3. Loss of interfering contrast as a function of mean number of photons spontaneously scattered by atoms within the interferometer. Each curve represents a different path separation: $d/\lambda = 0.06(\Delta)$, $0.13(\diamond)$, and $0.16(\circ)$.

The data follow a nearly exponential decay with \bar{n} . The non-exponential trend at large \bar{n} is a result of the finite size of our hot-wire detector which post-selects atoms within a limited range of transverse momentum. This has the effect of restricting the trace over final photon states to those which leave the atom with a momentum within the acceptance angle of the detector. We account for this by replacing κ in Eq. (9) with κ' where $1/\kappa'^2 = 1/\kappa^2 + 1/\kappa_d^2$ and $\kappa_d = 3.3(1)k_0$ is the momentum acceptance of our detector.

In the many photon limit, the decoherence function we have derived agrees with the solution to the master equation presented in the introduction. Comparing Eqs. (2) and (9), taking into account the time varying intensity profile, $I(t)$, of the scattering light as experienced by atoms in the beam, we identify: $\kappa^2 = D^2\tau$ where τ is the amount of time needed to scatter \bar{n} photons ($\bar{n} = \int_0^\tau \Gamma(I(t)) dt$). Because the atom-photon scattering interaction is well defined, and our decohering environment well controlled, we can accurately calculate the constant κ (equivalently D) for any given laser parameters.

Displayed in Figure 4 are data which demonstrate Gaussian reduction in contrast as a function of path separation for two different laser intensities. As before, we independently determined \bar{n} and σ_n for each intensity, and from these values along with κ_d we calculate $\kappa' = 2.5(1)k_0$ for the higher laser intensity and

$\kappa' = 1.8(1)k_0$ for the lower. Fitting the contrast data to Eq. (9) yields $\kappa' = 2.39(5)k_0$ and $\kappa' = 1.71(5)k_0$, within error of the calculated values.

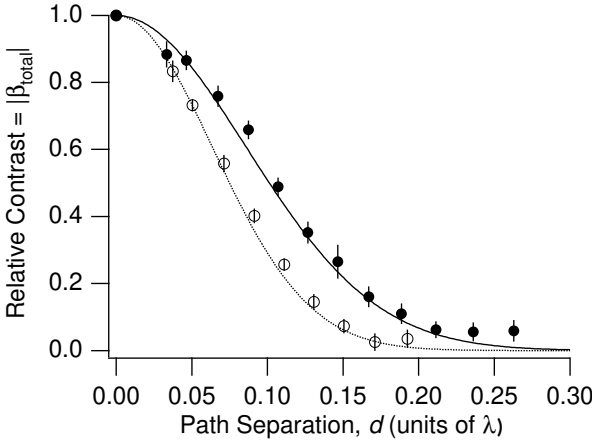


FIG. 4. Loss of contrast in the many-photon regime. Overlaid are theory curves generated from Eq. (9) using parameters (\bullet) $\bar{n} = 4.8(2)$, $\sigma_n = 1.8(1)$ and (\circ) $\bar{n} = 8.1(3)$, $\sigma_n = 3.5(1)$ determined from independent beam deflection measurements.

As with previous decoherence experiments [12,13], our system exhibits what have been referred to as the “naive” [10] generalizations of decoherence phenomenon: exponential loss of contrast with path separation squared and with number of scattered particles. The similarity of Eq. (1) to a diffusion equation [14], invites identification of this type of decoherence with phase diffusion or a random phase walk. To make the identification explicit, use the photon translation operator $e^{-i\hat{k}_x d}$ to rewrite the right hand side of Eq. (3) as:

$$|\psi\rangle_i \xrightarrow{\text{scat.}} |x\rangle \otimes |\phi_x\rangle + |x+d\rangle \otimes e^{ik_0 d} e^{-i\hat{k}_x d} |\phi_x\rangle = \int d\vec{k} \left(|x\rangle + e^{-i(k_x - k_0)d} |x+d\rangle \right) \otimes |\vec{k}\rangle \langle \vec{k}| |\phi_x\rangle \quad (11)$$

This expression for the entangled atom-photon wavefunction makes clear that if one were to measure the momentum of the scattered photon, the atom would then collapse into a superposition state with the phase between the two components shifted by an amount $\Delta\phi = (k_x - k_0)d$. Because the direction of the scattered photons is random, the phase of each atom’s interference fringes will vary, and their sum, the measured interference pattern, will have reduced contrast. This dephasing of atoms’ interference patterns is directly proportional to the atoms’ diffusion in transverse momentum: $\kappa\hbar$ is the rms spread in momentum transferred to an atom, and κd is the rms spread in phase of the atomic interference patterns.

In contrast, if one were to measure the position from which each photon had been scattered, Eq. (3) predicts that the atom will collapse into a superposition state with a reduced amplitude in one path, and increased amplitude in the other. Successive photons will continue this

process until only one component of the superposition has any remaining amplitude, that is, until complete which-path information has been obtained. When the experimenter is ignorant of the state of the scattered photons, whether an apparatus has been set up to measure them or not, the which-path and phase diffusion pictures are equally valid [15].

In conclusion, we have studied the decoherence of a spatial superposition due to photon scattering. Our data confirm theoretical predictions, and in the many-photon limit exhibit features of decoherence which are quite general (though not universal). We have observed the exponential coherence loss with time and path separation squared characteristic of this general behavior, and we have for the first time predicted and experimentally verified the decoherence rate constant κ . The particular model we have explored is not only the most relevant for macroscopic systems but also applies generally to situations in which decoherence arises slowly through a series of independent, mildly decohering interactions, the usual situation of interest for decoherence avoidance or correction protocols.

This work was supported by Army Research Office contracts DAAG55-98-1-0429 and DAA55-97-1-0236, Office of Naval Research contract N00014-96-1-0432, and National Science Foundation grant PHY-9877041.

- [1] W. G. Unruh, Phys. Rev. A **51**, 992 (1995).
- [2] H.-J. Briegel *et al.*, in *The Physics of Quantum Information*, edited by D. Bouwmeester, A. Ekert, and A. Zeilinger (Springer-Verlag, Berlin, 2000), pp. 281–293.
- [3] A. O. Caldeira and A. J. Leggett, Physica A **121**, 587 (1983).
- [4] W. G. Unruh and W. H. Zurek, Phys. Rev. D **40**, 1071 (1989).
- [5] E. Joos and H. D. Zeh, Z. Phys. B-Condens. Mat. **59**, 223 (1985).
- [6] M. R. Gallis and G. N. Fleming, Phys. Rev. A **42**, 38 (1990).
- [7] J. Schmiedmayer *et al.*, in *Atom Interferometry*, Vol. Advances in Atomic and Molecular Physics or *Advances in Atomic, Molecular and Optical Physics*, edited by P. Berman (Academic Press, San Diego, 1997), pp. 2–83.
- [8] T. Pfau *et al.*, Phys. Rev. Lett. **73**, 1223 (1994).
- [9] M. S. Chapman *et al.*, Phys. Rev. Lett. **75**, 3783 (1995).
- [10] J. R. Anglin, J. P. Paz, and W. H. Zurek, Phys. Rev. A **55**, 4041 (1997).
- [11] C. C. Cheng and M. G. Raymer, Phys. Rev. Lett. **82**, 4807 (1999).
- [12] M. Brune *et al.*, Phys. Rev. Lett. **77**, 4887 (1996).
- [13] C. J. Myatt *et al.*, Nature **403**, 269 (2000).
- [14] W. H. Zurek, Phys. Today **44**, 36 (1991).
- [15] A. Stern, Y. Aharonov, and Y. Imry, Phys. Rev. A **41**, 3436 (1990).